



# Lightning, overshooting top and hail characteristics for strong convective storms in Central Europe

Petra Mikuš Jurković\*, Nataša Strelec Mahović, Damir Počakal

Meteorological and Hydrological Service, Zagreb, Croatia



## ARTICLE INFO

### Article history:

Received 18 July 2014

Received in revised form 24 March 2015

Accepted 27 March 2015

Available online 23 April 2015

### Keywords:

Convection

Lightning

Overshooting tops

SEVIRI brightness temperature differences

Hail characteristics

## ABSTRACT

Lightning activity in storms with overshooting tops and hail-producing storms over Central Europe is studied, in order to find typical lightning characteristics that can be useful in nowcasting of the severity of the storm and its ability to produce hail. The first part of the study gives the analysis of lightning activity in thunderstorms with overshooting tops (OT) for the warm part of the year (May–September) from 2009 to 2010 over central and southeastern Europe. Deep convective clouds with OT were detected in Meteosat Second Generation (MSG) Spinning Enhanced Visible and Infrared Imager (SEVIRI) data, using methods based on the infrared window (IRW, 10.8 μm) channel and absorption channels of water vapor (WV, 6.2 μm) and ozone (O<sub>3</sub>, 9.7 μm) in the form of brightness temperature differences. The locations and times of the detected OT were compared to the distribution and types of lightning strokes, which were provided by the LINET Lightning Location System. The results show that the spatial distribution of lightning generally coincides with the spatial distribution of the detected OT. The largest numbers of lightning strokes and OT were found in western Hungary, southeastern Austria, northeastern Slovenia and the northern Adriatic. The largest number of OT occurred between 1600 and 1800 UTC, whereas from 0600 to 1000 UTC OT detections were rather rare. Lightning activity showed a similar temporal distribution, with an increase in lightning activity evident at or close to the time of the OT detections. At the time of and close to the location of the OT, the lightning was found to occur well above the tropopause and was clearly related to the OT of cumulonimbus clouds.

In the second part of the study, lightning characteristics are studied for 35 events of hail-producing thunderstorms over Croatia in the summer months (May to September), from 2008 to 2012. The lightning distribution, also registered by LINET, was compared to hail parameters based on measurements at the hailpad polygon. A polygon with dimensions of 30 km × 20 km was located in the area of highest average number of days with hail occurrence in the continental part of Croatia. In a majority of the studied cases, the number of total lightning strokes sharply increased slightly before the beginning of hailfall. At the time the hailfall started there is a brief decrease in the number of lightning strokes, followed by a sharp increase shortly after. Additionally, larger hailstones with higher kinetic energy values appeared at the beginning of the hailshower. Microphysical properties of the cloud tops, investigated using MSG SEVIRI 3.9 μm reflectivity, i.e. profiles of the effective radii of cloud particles vs. temperature, clearly verify the presence of strong updrafts associated with hail-producing clouds.

© 2015 Elsevier B.V. All rights reserved.

## 1. Introduction and background

The updraft area of a severe thunderstorm is frequently manifested by the appearance of the overshooting tops (OTs). Generally, the largest OTs, with diameters of up to 15 km and lifetimes of several hours, are usually detected within the strongest storms. These storms often produce hazardous weather conditions, such as large hail, damaging wind, heavy rainfall and tornados with significant consequences on the Earth's surface (Bedka, 2010; Setvak et al., 2010; Dworak et al., 2012). In addition to the hazardous weather conditions on the ground, storms with OTs have also been associated with strong horizontal and

vertical wind shear and frequent lightning (Wiens et al., 2005; Machado et al., 2009; Meyer et al., 2013) and generate significant near-storm turbulence, which is a consequence of gravity wave generation at storm top (Wang et al., 2010) and subsequently represent a serious risk for aircraft. The OT and cold ring features can be indicators of severe thunderstorms that usually produce large hail, severe wind and possibly tornadoes (Iršič Žibert and Žibert, 2012; Mikuš and Strelec Mahović, 2012b). Because of the significant correlation between the occurrence of an OT and severe weather conditions on the ground (Bedka, 2010; Mikuš and Strelec Mahović, 2012b; Dworak et al., 2012), as well as aircraft accidents caused by convectively induced turbulence (Cornman and Carmichael, 1993), OT detection has become more important in operational nowcasting. OT are most easily observed in high resolution visible (HRV) images that are limited to daytime

\* Corresponding author.

E-mail address: [petra.mikus@cirrus.dhz.hr](mailto:petra.mikus@cirrus.dhz.hr) (P. Mikuš Jurković).

hours and depend on the sun angle, OT heights and shadow lengths, time period of the OT observation, and experience of the forecasters. In color enhanced infrared (IRW, 10.8 μm) satellite images, OTs are usually represented with a relatively small group of pixels colder than the surrounding pixels of the convective cloud anvil (Bedka et al., 2010). However, sometimes OTs are not represented with a brightness temperature (BT) minimum, especially in storms with specific thermal features at the cloud top, such as cold ring or cold U/V (Stastka and Setvak, 2008). Because of these visual detection limitations, objective satellite-based OT detection methods have been developed that represent helpful nowcasting tools, especially for regions that lack radar coverage. The objective OT detection methods are usually satellite based (Rosenfeld et al., 2008; Bedka et al., 2010; Mikuš and Strelec Mahović, 2012b), but the recognition and detection of OT in satellite imagery are strongly dependent on the spatial and temporal resolution of the satellite instruments, and for those methods that rely on visible satellite imagery possible only during daytime.

OTs are linked to the electrical activity of the storm, since updraft surges coincide with an increase in total flash rate (Wiens et al., 2005). The specific behavior of lightning discharges during thunderstorms with OT was found in several investigations (Elliot et al., 2012) and suggested that the amount of lightning within a convective cloud can improve the detection of the OT. In order to include lightning data in an objective detection method over central Europe, an analysis of lightning activity in convective clouds with OT is required, aiming to define the important criteria and thresholds. In Section 3.1 the total number of lightning strokes along with their spatial and temporal distributions (in general and separately in penetrative convective clouds) is analyzed over central and southeastern Europe. The number, type and peak currents of lightning strokes in convective clouds with OT are then shown for several cases.

A rapidly growing flash rate has been related to an increase in the potential for severe weather (Williams et al., 1999), yet does not guarantee that severe weather will occur. During severe thunderstorms, cloud-to-ground (CG) lightning production appears to decrease, whereas a significant increase in the number of intra-cloud (IC) flashes is registered (MacGorman, 1993; Buechler et al., 1996; Lang et al., 2000 and Lang and Rutledge, 2002; Emersic et al., 2011). In hailstorms, regions with a reduced number of lightning strokes, called lightning holes, have been observed (Emersic et al., 2011). These regions are usually short lived and are related to wet hail growth that is not conducive to hydrometeor charging (Emersic et al., 2011; Lynn et al., 2012), or in the case of supercell storms, the consequence of a strong rotating updraft (MacGorman et al., 2008). Many previous studies of thunderstorms have shown that graupel and ice crystals are the species that are the most important in the electrification of storms and the occurrence of lightning (Black and Hallett, 1999; Bruning et al., 2007). Carey and Rutledge (1998) compared hail and CG lightning trends and showed that in certain cases, the maximum of CG lightning activity occurs after hail occurrence, while Soula et al., (2004) found very weak CG lightning activity during the severe hailstorms. The studied hail-producing storms in their mature phases sometimes produced more positive CG flashes, while production of negative CG flashes was very low (Soula et al., 2004; Montanya et al., 2007, 2009; Dimitrova et al., 2013). Furthermore, the total flash rate rapidly increases before severe weather occurrence, such as large hail, severe wind or tornadoes (Schultz et al., 2009, 2011; Darden et al., 2010; Gatlin and Goodman, 2010). Dimitrova et al., (2013) observed significant jump in total flash rate before the beginning of the hail fall. Previous studies also showed significant increase of IC lightning activity and IC/CG ratio before the occurrence of severe weather at the ground (Montanya et al., 2007, 2009). Therefore, total lightning information is considered to be one of the best early indicators of a strengthening updraft within a thunderstorm (Schultz et al., 2011).

Another measure of the intensity of a convective storm's updraft, and hence its ability to produce large hail, is the vertical evolution of

cloud-top microphysical features (Lensky and Rosenfeld, 2006; Rosenfeld et al., 2008). A conceptual model is presented that assesses the intensity of severe convective storms by using satellite-retrieved vertical profiles of cloud top temperature vs. particle effective radii ( $T-r_e$  profiles), whereas deep clouds composed of small particles at cloud top ( $r_e$ 's of 15–20 μm) are associated with greater updraft velocities and very cold supercooled drops to below –30 °C. Rosenfeld et al. (2008) further analyzed a large number of severe hail-producing storms and showed that stronger updrafts are revealed by the delayed growth of particle  $r_e$  to greater heights and lower temperatures.

The present study is divided into two parts. The first part, given in Section 3.1 is dealing with distribution and general properties of lightning activity over Central Europe in correlation to OT occurrence. In the second part of the study (Section 3.2), spatial and temporal characteristics of lightning are studied for thunderstorms producing hail over a hailpad polygon located in the northwestern part of Croatia. Additionally, for the studied hailstorm cases, hail characteristics, such as the hailstone diameter and kinetic energy, as well as  $T-r_e$  profiles were analyzed. Finally, the main findings and conclusions are summarized in Section 4.

## 2. Data and methods

Over the central European domain (Fig. 1a), an analysis of lightning activity in thunderstorms with OT was performed using the lightning data provided by the low-frequency (VLF/LF) International Lightning Detection Network (LINET). For general analysis of the spatial distribution, the number of detected lightning strokes was calculated over  $0.2^\circ \times 0.2^\circ$  grid boxes. Detailed analysis of lightning activity was done for selected convective episodes. The convective cells were tracked during their lifetime and only the lightning activity connected to the tracked cell was analyzed. LINET system covers a wide area from approximately 30°N 10°W to 65°N 35°E and detects the total lightning, but it also separately detects CG strokes and IC discharges (Betz et al., 2009; Mikuš et al., 2012). LINET intra-cloud detections will be termed "IC-strokes" according to the terminology given by Betz et al. (2004). This technical term is used to emphasize the distinction from IC radio sources detected with VHF sensors and should not be confused with CG return strokes. Detection efficiency of LINET sensors is very high, enabling detection of strokes with peak currents below 5 kA. Statistical average location accuracy is better than 150 m (Betz et al., 2009); however the sensitivity of the sensors decreases as the distances of the lightning strokes from the LINET sensors increase (Höller et al., 2009). The discrimination between IC and CG lightning strokes is possible by using the three dimensional time-of-arrival (TOA) analysis (Betz et al., 2004). For the reliable determination of the IC strokes height, at least 4 sensors are needed, located within 150–200 km of each other (Betz et al., 2009). In the central part of the network even very weak lightning events can be detected (<5 kA) and discrimination between CG and IC lightning is more successful than in the surrounding areas, where the sensors detect predominantly stronger events such as CG strokes (Dimitrova et al., 2013; Betz et al., 2009). Over the studied domain lightning is detected by approximately 40 sensor sites.

OTs of the deep convective clouds were detected from the Meteosat Second Generation (MSG) Spinning Enhanced Visible and Infrared Imager (SEVIRI) data with a sampling distance of 3 km per pixel (Schmetz et al., 2002) and 15 minute temporal resolution, using a 'COMB' method (Mikuš and Strelec Mahović, 2012b). The 'COMB' method is based on the infrared window (IRW, 10.8 μm) channel and the absorption channels of water vapor (WV, 6.2 μm) and ozone ( $O_3$ , 9.7 μm) in the form of brightness temperature differences (BTD). It combines the criteria for the IRW brightness temperature (BT) and criteria for the two BTDs, WV-IRW and  $O_3$ -IRW. All pixels with  $O_3$ -IRW BTD larger than 13 K in the region where the IRW BT is lower than 215 K and WV-IRW BTD is larger than 4 K are characterized as OT. Additionally, the 'COMB' method is strongly dependent upon the spatial resolution of



**Fig. 1.** a) Surface elevation map of the study domain (green colors represent lower and brownish colors higher values of elevation). Black lines indicate the political borders. b) Location of the hailpad polygon in the northwestern part of Croatia. Dashed line denotes the state border with Slovenia and Hungary. Cities in the vicinity of the polygon are marked.

the satellite instruments, which implies that certain OT can be recognized in the 1 km resolution HRV imagery but cannot be detected using the BTD method based on SEVIRI data with spatial resolutions of 3 km (Mikuš and Strelec Mahović, 2012b). All pixels in one MSG SEVIRI scan within the range of 0.1° (approx. 10 km) from the position of the

pixel with the lowest IR BT that met the COMB criteria for OT are defined as one OT detection. This box criterion was selected because the largest OT diameter according to previous studies (Brunner et al., 2007; Bedka et al., 2010) was approximately 12 km. Additionally, this criterion considers the possible errors in the COMB BTD method, which in certain

cases detects too large an area to exclusively represent one OT (Mikuš and Strelec Mahović, 2012b). The geographical coordinates of the pixel with the lowest IR BT that met the COMB criteria for OT represented the location of detected OT.

The number of detected OT was calculated over  $0.2^\circ \times 0.2^\circ$  grid boxes for the analysis of the spatial distribution of OT. For the temporal distribution of the detected OT, the number of OT detections was calculated every 15 min, i.e. at the time of the satellite scan which is app. 11 min after the nominal satellite time. For the analysis of the temporal distribution of the lightning strokes, detected lightning strokes were grouped into 15 minute bins, where the number of strokes at the time of satellite scan represented a total number of all detected strokes during the time interval  $\pm 7.5$  min from the time of a certain satellite scan.

Additionally, for every satellite-based detection of OT, the occurrence of the lightning discharges was searched during the period starting 7.5 min before and ending 7.5 min after the time of the satellite scan (app. 11 min after the nominal satellite time) over the area of interest within the range of  $0.1^\circ$  from the OT pixel position. In other words if the OT is detected in the satellite data with nominal time 1200 UTC, it is considered that this detection occurred over the area of interest at 1211 UTC, and the lightning discharges connected to that OT were searched in the period from 7.5 min before to 7.5 min after that time within the range of  $0.1^\circ$  from the center of the pixel which was recognized as OT. In case there were several OTs detected close to each other we made sure that each lightning stroke is assigned to only one OT, i.e. we did not count the same stroke more than once. The number of these lightning discharges was then calculated over  $0.2^\circ \times 0.2^\circ$  grid boxes.

For the 35 hail-producing thunderstorms occurring over northwest Croatia in summer months (May to September) from 2008 to 2012, the lightning distribution was compared to hail occurrences based on the data collected from a hailpad polygon (Počakal, 2011). The polygon consisted of 150 hailpads (Fig. 1b) and covered an area of  $\sim 600 \text{ km}^2$  with an approximate distance between hailpads of up to 2 km. A hailpad is a simple meteorological device used for hailstone recording that was developed and used by Scheusener and Jennings (1960). It consists of a stand and a measuring plate. The working principle is based on measuring the size of a trace that hailstone leaves when hitting the plate. The main parameter that can be determined from one hailpad, in addition to the number and diameter of hailstones, is the intensity (kinetic energy) of hail, which is calculated using the method of Mezeix and Doras (1981).

All studied hailstorms were checked for the appearance of OT using the COMB method and verified in HRV images where available. Color-enhanced IRW 10.8  $\mu\text{m}$  satellite images were also analyzed to determine the IRW BT and specific thermal signatures of convective clouds with OT. In the convective storm examples presented in this paper the storm top characteristics were additionally studied using the rapid scan satellite data, which are in 5 min intervals. For cases with apparent OT, detailed analyses of the lightning properties and physical properties of hailstones on the ground (number, diameter and kinetic energy) were then performed. Lastly, for the hail-producing storms registered by the hailpads, the cloud-top microphysical properties were analyzed by means of MSG SEVIRI 3.9  $\mu\text{m}$  reflectivity in form of T- $r_e$  profiles (vertical profiles of cloud top temperature vs. particle effective radii). Based on the properties of the 3.9  $\mu\text{m}$  channel, the vertical evolution of the cloud top particle size can be retrieved using the methodology of Rosenfeld and Lensky (1998). They related the retrieved  $r_e$  to the temperature (T) of the convective cloud tops. The maximum detectable  $r_e$  is 35 mm because the signal saturates at higher values. The T- $r_e$  relations are obtained from reflectivity information that is retrieved from the 3.9  $\mu\text{m}$  channel from clouds over range of top temperatures. The methodology of Lensky and Rosenfeld (2006) assumes that the T- $r_e$  relations obtained from a scene of clouds at various stages of their development equals the T- $r_e$  evolution of the top of a single cloud as it grows vertically. The limitation of the method is the availability of the 3.9  $\mu\text{m}$  reflectivity only during the day.

### 3. Results

#### 3.1. Characteristics of lightning activity in deep convective clouds with the OT

##### 3.1.1. Spatial and seasonal analysis

For the study period, the largest numbers of lightning strokes were detected in western Hungary, southeastern Germany and Austria, the northern Adriatic and northeastern Slovenia. The minimum lightning

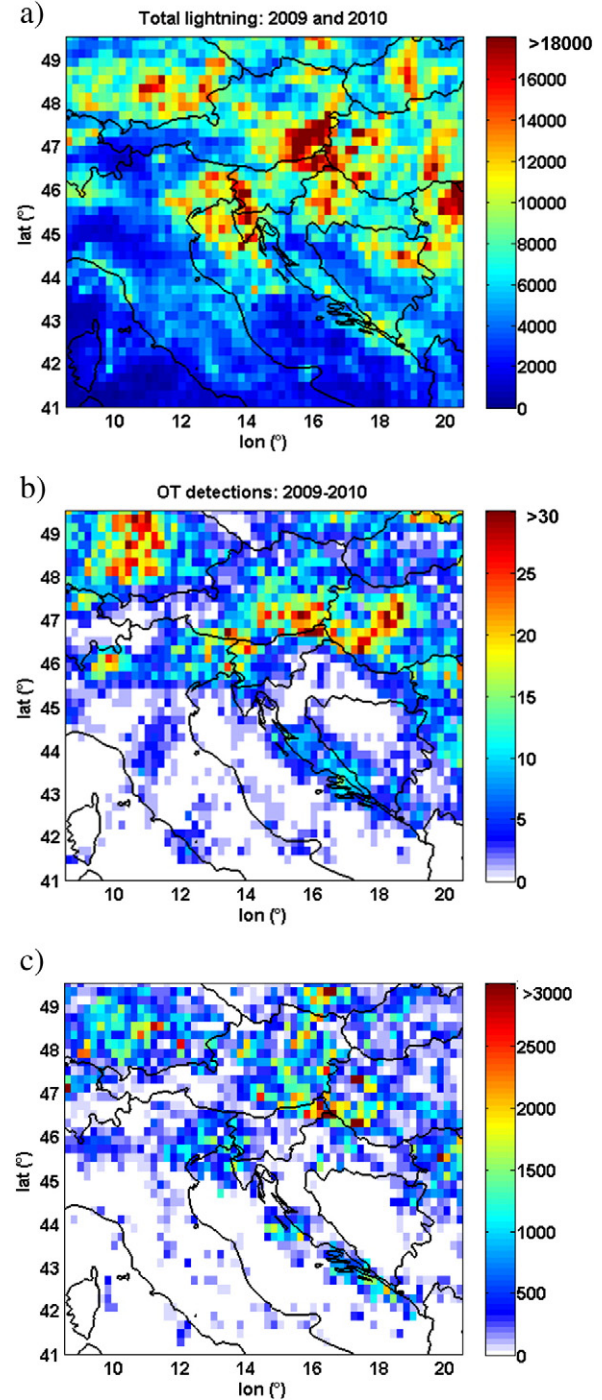


**Fig. 2.** a) Spatial distribution of total (IC + CG) lightning strokes computed over  $0.2^\circ \times 0.2^\circ$  grid boxes and b) number of OT detections using COMB method computed over  $0.2^\circ \times 0.2^\circ$  grid boxes from May to September 2009 and 2010. c) Number of lightning strokes 7.5 min before and after the time of the satellite scan within the range of  $0.1^\circ \times 0.1^\circ$  from the OT position. Spatial distribution is computed over  $0.2^\circ \times 0.2^\circ$  grid boxes.

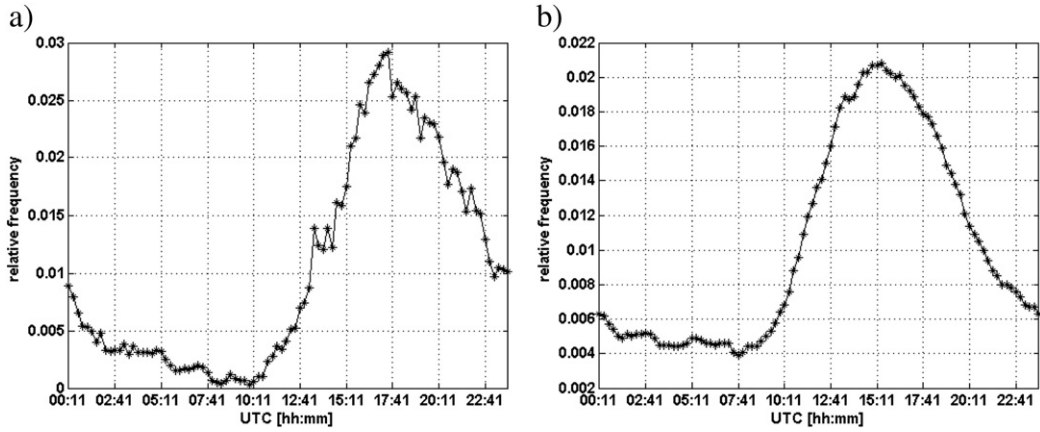


**Fig. 3.** Relative frequency of a) OTs detected using COMB method and b) lightning strokes, both calculated every 15 min, i.e. at the time of the satellite scan (app. 11 min after the nominal satellite time). Detected lightning strokes are grouped into 15 min bins, where number of strokes at the time of satellite scan represents a total number of all detected strokes during the time interval  $\pm 7.5$  min from the time of certain satellite scan.

activity occurs over the highest tops of the Alps and Dinaric Alps as well as over the Adriatic Sea (Fig. 2a). This is generally consistent with a previous study of the lightning activity in Croatia during the warm seasons

in 2006–2009 reported by Mikuš et al. (2012), who noted that the minimum lightning activity is found in mountainous areas, whereas over the sea, lightning often appears close to the coastline.

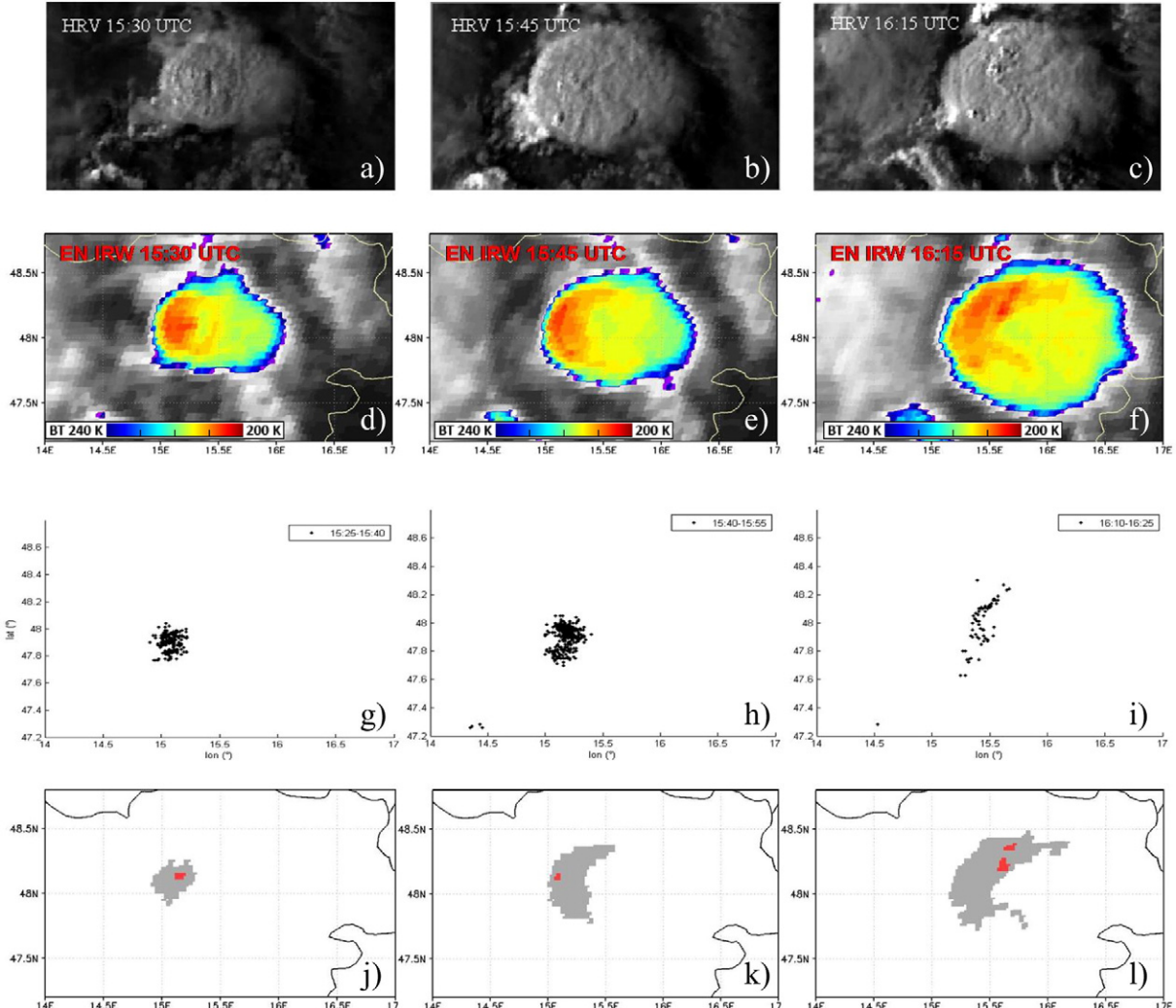


**Fig. 4.** Meteosat 9 HRV channel imagery on 23 August 2010 at a) 15:30, b) 15:45, c) 16:15 UTC, and color-enhanced Meteosat 9 10.8  $\mu$ m imagery at d) 15:30, e) 15:45, f) 16:15 UTC. Map of IC lightning activity above 12 km (tropopause level) at g) 15:25–15:40 h) 15:40–15:55 and i) 16:10–16:25 UTC for the analyzed convective storm region. Pixels meeting the criteria (red) for the BT (<215 K), WV-IRW (>4 K) and O3-IRW (>13 K) for the studied convective storm at j) 15:30 UTC, k) 15:45 UTC and l) 16:15 UTC. Gray pixels in Fig. 4j, k and l indicate area where BT is lower than 215 K, WV-IRW > 2 K and O3-IRW > 10 K. Note: The differences between locations of surface lightning data and cloud tops in the satellite images are caused by the parallax shift.

The highest frequency of lightning occurrence over the continental part of the studied region was recorded during July in 2009 and 2010, whereas the convective activity over the sea is more pronounced in the autumn (not shown), which is also consistent with previous studies of lightning activity over Europe (Christian et al., 2003; Schulz et al., 2005; Mikuš and Strelec Mahović, 2012a). From May to August most of the lightning activity occurred over the continental portion of the study area, while in September the lightning activity was more pronounced along the coastline and over the sea (Anderson and Klugmann, 2014). This was most likely associated with the increased cyclonic activity across the Mediterranean Sea during the autumn months and increased temperature contrast between the warmer sea surface and colder European air masses, which is suitable for convection development (Manzato, 2007). Although not analyzed in detail here, the lightning activity was significantly lower in the cold season from November–April because of unfavorable weather conditions for the development of convection (Anderson and Klugmann, 2014).

A significant number of OT detected using the COMB BTD satellite-based detection method were found at the slopes of the Alps in southeastern Austria and Germany, as well as in northern Italy (Fig. 2b). The maximum number of OT during the analyzed warm seasons was detected in central Hungary. During May, the OTs were usually detected over the land areas, with maximum activity during June and July. In September, the OT activity increased along the coastline and over the sea (not shown), which was also described in the study performed by Bedka (2010). In regions with significant lightning activity (southeastern Austria, eastern Slovenia, western Hungary and Slovenia) (Fig. 2a), the highest number of OT was also detected (Fig. 2b). Schulz et al.

(2005) analyzed CG lightning activity from 1992–2001 and found that the locations of the maximum OT detections are consistent with the maxima in CG lightning activity. Less correlation between spatial distributions of total lightning strokes (Fig. 2a) and detected OT (Fig. 2b) was noted in southeastern Germany. The region in southeastern part of Germany with the strongest lightning activity does not have large number of detected OT, but mature convective clouds seem to have been producing significant lightning activity in the vicinity of detected OT (Fig. 2c).

Fig. 2c displays the spatial distribution of the number of lightning strokes detected during the interval from 7.5 min before to 7.5 min after the time of the satellite scan (which is app. 11 min after the nominal time of the satellite scan) over the area of interest, within the range of  $0.1^\circ$  from the OT position. It shows that a significant number of total lightning strokes were registered in the vicinity of the OT. The maximum number of approximately 9500 lightning strokes in  $0.2^\circ \times 0.2^\circ$  grid box (app. 45% of all detected lightning strokes) was detected in Hungary. Additionally, in the southern Adriatic coastal region at the slopes of the Dinaric Alps, a significant amount of lightning (app. 30% of all detected strokes) was detected in the vicinity of the detected OT.

### 3.1.2. Temporal analysis

OTs were more frequently detected during the daytime from 0900 to 2100 LST (Local Standard Time; UTC + 2 h) than the nighttime from 2100 to 0900 LST (Fig. 3a), especially near the slopes of the mountains, which is consistent with the results described by Bedka (2010). Comparably, daytime lightning activity strongly dominated over the nocturnal lightning events in the continental regions. The nocturnal

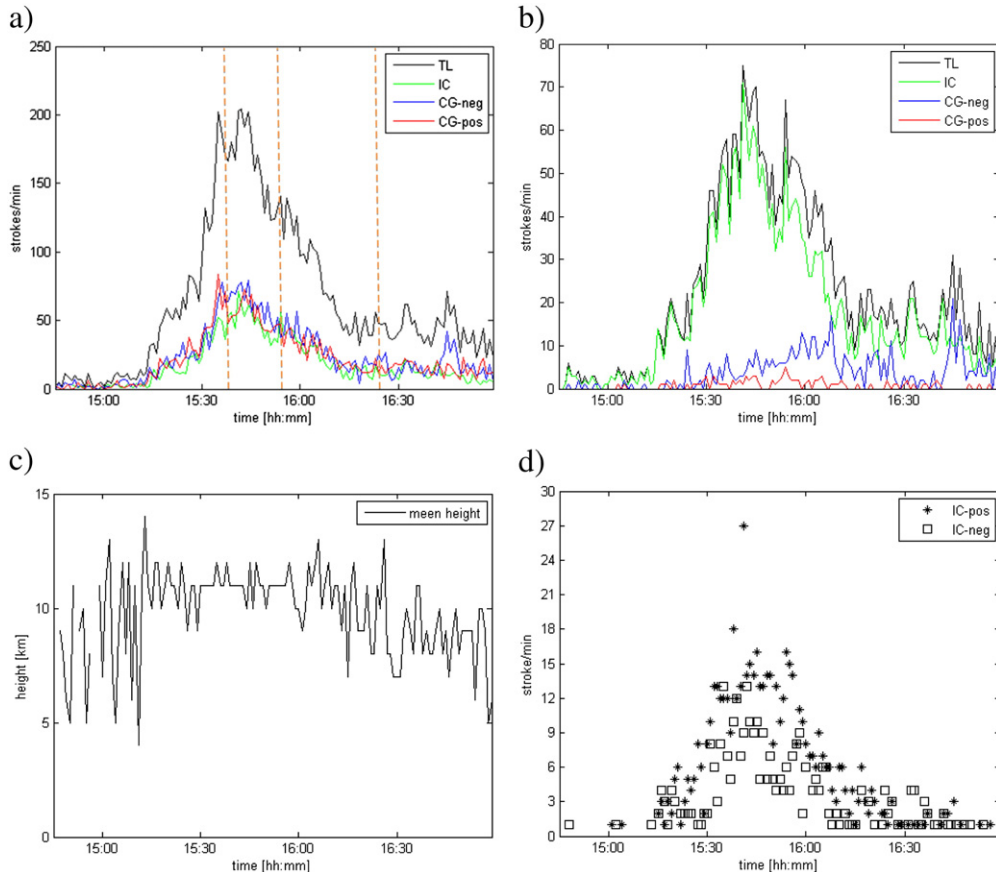


**Fig. 5.** Temporal distribution of a) lightning strokes (CG positive, CG negative, IC and TL) and b) filtered lightning strokes (CG positive > 10 kA, CG negative > 10 kA, IC and TL). c) Mean height of IC lightning strokes, d) polarity of IC strokes above 12 km on 23 August 2010. Dashed lines (Fig. 5a) indicate approximate time of the OT detections on Meteosat 9 HRV channel imagery shown in Fig. 4a, b and c.

**Table 1**

Number of hail-pads on which the hail was registered, start and end time of hailfall over the hail-pad polygon, hail characteristics such as maximum radius (Max. radius) and maximum kinetic energy (Max. KE) of the hail stones for analyzed hail storms. T-r<sub>e</sub> vertical profiles were done only for the day-time thunderstorms (shaded rows). Occurrence of OT and cold ring (U/V) feature over or near to the hail-pad polygon are indicated.

Date	No. of hail-pads	Start time (UTC)	End time (UTC)	Max.radius (mm)	Max.KE ( $\text{Jm}^{-2}$ )	OT	Cold U/V
06.05.2008	1	15:12	15:15	7.7	3.0	+	–
30.05.2008	13	18:05	18:35	25.0	66.0	+	+
03.06.2008	2	06:47	08:15	10.6	12.1	–	–
11.06.2008	5	15:45	16:32	16.3	41.6	–	–
17.06.2008	38	14:40	15:30	22.4	284.4	+	–
24.06.2008	7	19:30	19:46	16.0	36.6	+	–
27.06.2008	9	17:30	18:30	25.1	193.4	+	–
07.07.2008	13	19:50	20:10	21.5	51.6	+	–
14.07.2008	15	05:20	06:30	24.3	211.9	–	–
02.08.2008	2	14:45	15:10	10.8	13.9	+	+
08.08.2008	1	13:55	13:57	5.8	0.3	+	–
15.08.2008	6	21:05	21:43	13.5	48.9	+	–
15.08.2008–16.08.2008.	7	23:00	00:02	13.1	59.6	–	–
23.08.2008	2	15:15	15:39	10.8	16.6	–	–
03.05.2009	1	14:30	14:33	7.0	1.3	–	–
04.05.2009	1	15:15	15:25	9.1	2.9	–	–
24.05.2009	4	21:30	21:32	11.0	6.9	+	–
26.05.2009	1	20:45	20:55	13.6	5.0	–	–
29.05.2009	1	14:45	14:47	6.8	0.3	–	–
10.06.2009	4	13:25	13:35	14.1	8.9	–	–
11.06.2009	3	15:25	15:30	10.4	3.5	–	–
05.07.2009	2	14:25	14:30	9.7	8.2	+	–
17.06.2010	1	19:05	19:10	10.6	16.8	+	+
04.07.2010	1	18:43	18:45	10.4	3.2	–	–
03.08.2010	3	15:20	15:40	15.5	15.3	–	–
01.05.2011	2	14:58	15:10	6.8	5.8	–	–
21.05.2011	1	14:55	15:05	10.0	1.0	+	–
24.05.2011	3	13:20	13:45	12.7	62.0	–	–
01.06.2011	1	14:20	14:25	7.3	2.7	–	–
01.06.2011	2	19:15	19:25	12.7	72.0	+	–
07.06.2011	1	19:58	20:03	8.8	1.5	–	–
19.08.2011	1	15:57	16:05	10.4	0.9	–	–
23.05.2012	13	15:10	15:30	18.2	47.7	+	–
24.05.2012	9	15:45	16:03	17.7	31.0	–	–
11.07.2012	14	22:30	22:55	23.2	162.6	+	–

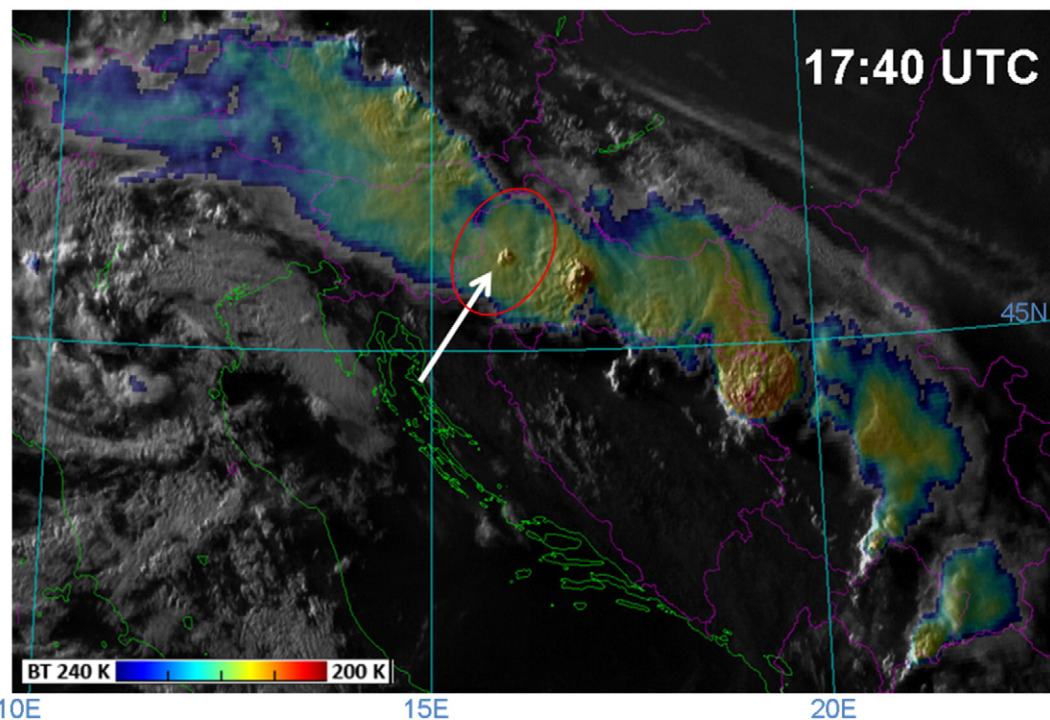


**Fig. 6.** Meteosat 8 "Sandwich" product (HRV image overlaid with color-enhanced MSG IR 10.8  $\mu\text{m}$  image) for 30 May 2008, 17:40 UTC. OT closest to the hailpad polygon is marked by an arrow. Tracked and analyzed convective cell was allocated using lightning and satellite data. The analyzed cell is marked with the red curved line.

lightning occurrence was more common over the coastal regions, especially during September (Mikuš et al., 2012). Between 0600 and 1000 UTC, the OT detections and lightning discharges were not frequent (Fig. 3). A comparison of the temporal distribution of the frequency of OT detections and lightning strokes showed differences, especially from 0000 to 1200 UTC. During nighttime and morning, the relative frequency of the OT was much lower than the frequency of lightning strokes. A possible explanation is that during nighttime in the summer months, convection was often triggered over the sea and along the coastline (Mikuš et al., 2012) where convective activity was usually weaker compared to that over the continental areas (Ávila et al., 2010). Consequently, lightning strokes during the nighttime and morning were usually a product of the convective clouds with updrafts that were not strong enough for significant OT development. In general, the largest number of OT occurred during the afternoon and early evening (Fig. 3a), with well-pronounced peaks between 1626 and 1726 UTC in association with the time period of very high atmospheric instability (Bedka, 2010). Temporal analysis of the occurrence of lightning discharges (Fig. 3b) showed that the largest number of lightning strokes for the study area during the analyzed warm seasons usually occurred from 1300 to 1800 UTC, with the highest lightning activity between 1426 and 1626 UTC. This diurnal variation of lightning activity followed the diurnal, radiatively forced heating cycle of the atmospheric boundary layer (Stull, 1988). During the time period with maximum number of OT detections, lightning activity was very strong, suggesting that they are both good indicators of deep, moist convection as discussed before (Ávila et al., 2010). It should be noted that in case of severe convective storms, the OT might appear with a frequency of <5 min, even <2 min; therefore, these OTs are missed if only 15 min imagery is used for the detection. Despite this slight discrepancy, the overall appearance of the temporal changes in lightning activity is comparable to the temporal distribution of the OT frequency.

### 3.1.3. Characteristics of lightning strokes

Lightning types, frequencies and polarities are related to microphysical and dynamical processes within storms, and can supply important information on the development and intensity of particular storms (Perez et al., 1997; Williams et al., 1999; Buechler et al., 2000; Tuomi and Larjavaara, 2005; Darden et al., 2010). The most obvious and systematic characteristic of thunderstorms with OT is a rapid increase in total lightning flash rate, which often occurs at the time or less than 5 min before OT detections (Emersic et al., 2011; Rogers et al., 2013). Previous studies have also found that thunderstorms with stronger updrafts have the potential to produce more lightning (Boccippio, 2002). Similarly, Williams et al. (1999) observed an abrupt increase in flash rate just before severe weather occurred at the ground for Florida thunderstorms, while numerous other studies have also found positive correlations between rapid increases in total lightning and manifestations of severe weather at the surface (Bridenstine et al., 2005; Wiens et al., 2005; Steiger et al., 2005, 2007; Gatlin, 2006; Montanya et al., 2007, 2009; Dimitrova et al., 2013). A characteristic of severe thunderstorms is a decrease in the CG lightning production with a subsequent and significant increase in the number of IC flashes (Maddox et al., 1997; Steiger et al., 2005; Tessendorf et al., 2007; Schultz et al., 2011). Severe storms have been shown to at times possess exceptionally low negative CG flash rates (Soula et al., 2004; Montanya et al., 2007) because the strong updrafts during these thunderstorms result in high IC flashes and, in some cases, positive CG flashes (Lang et al., 2000). Previous studies have also shown that the CG flash rate is not adequate for predicting severe storm development, especially in cases of tornado genesis (Perez et al., 1997; Williams et al., 1999; Tuomi and Larjavaara, 2005). Therefore, total lightning information is considered to be one of the best early indicators of a strengthening updraft within the thunderstorm and the potential for severe weather occurrences.

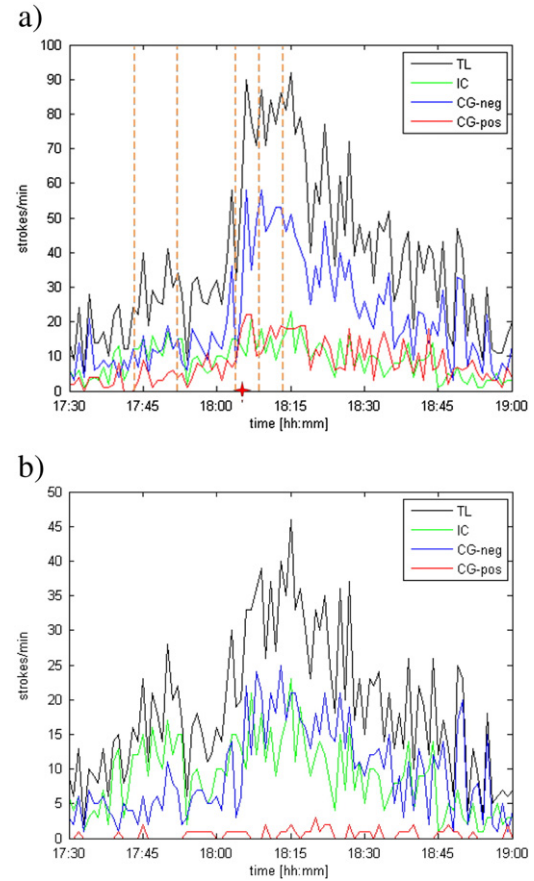


**Fig. 7.** Temporal distribution of a) lightning strokes (CG positive, CG negative, IC and TL) and b) filtered lightning strokes (CG positive > 10 kA, CG negative > 10 kA, IC and TL) on 30 May 2008. Dashed lines indicate approximate times of the OT detections: 1740, 1750, 1800, 1805 and 1810 UTC nominal time of satellite scans. Star indicates beginning of the hailfall detected over the polygon (1805 UTC).

For the analyzed period, in addition to documenting larger total lightning flash frequencies, larger values of electric current were found slightly before the time of OT detections. Lightning was found to occur well above the tropopause and was clearly related to the OT parts of the cumulonimbus cloud, which protrude through the storms' equilibrium level and often penetrate into the lower stratosphere (Lane et al., 2003; Wang, 2007; Setvak et al., 2010).

The characteristics of the lightning activity during thunderstorms with OT are shown in an example of a convective storm on 23 August 2010 (Fig. 4a–l). The OTs were well pronounced on the HRV satellite

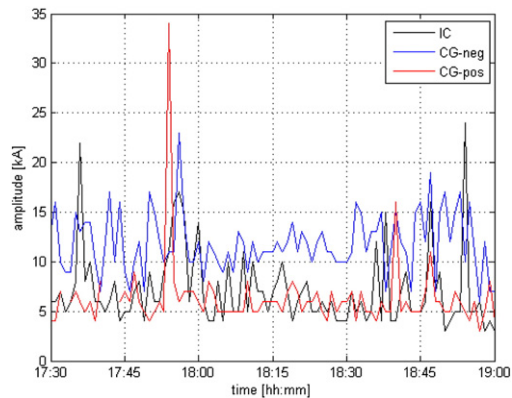


**Fig. 8.** Mean amplitude (kA) of CG positive, CG negative and IC peak currents on 30 May 2008.

imagery in the period between 1530 UTC and 1615 UTC (Fig. 4a–c) and were detected using the COMB BTD detection method (Fig. 4j–l). The so-called ‘cold ring’ structure visible in the enhanced IR 10.8 μm satellite image (Fig. 4d) was recognizable as the central warm spot (light green to yellow in Fig. 4d) surrounded by the colder ring-shaped region (red in Fig. 4d). This kind of cold/warm couplet on the top of the storm indicates the possible severity of the storm (Iršič Žibert et al., 2010). In Fig. 4e and f, the warm spot was not entirely enclosed within the cold part and formed a ‘cold U/V’ thermal feature. These specific thermal features resulted from the OT and formed because of the favorable atmospheric conditions in which the key factors for their development are storm-top-level wind shear and an above-tropopause inversion (Setvak et al., 2010).

An analysis of the lightning characteristics was performed for all of lightning strokes that were detected along the track of the convective cell with specific thermal features on the storm top (Fig. 4). A sharp increase in the number of lightning strokes (Fig. 5a and b) was evident at the time of the OT detections. Starting at 1530 UTC the number of total lightning strokes increased continuously, reaching the maximum

number of 202 strokes per minute at 1535 UTC (Fig. 5a). That is the period of very strong convective activity resulting with OT and cold ring feature visible in the satellite images (Fig. 4a–c). After 1542 UTC the number of total lightning strokes started to decrease. Separate numbers of CG +, CG – and IC strokes, showed very similar behavior during the lifetime of the studied convective cell (Fig. 5a). This storm produced a significant number of CG + lightning strokes (2993 strokes between 1445 UTC and 1700 UTC), indicating the severity of the storm (Soula et al., 2004; Wiens et al., 2005). The production of CG + strokes was almost the same compared to CG – strokes (3268 strokes between 1445 UTC and 1700 UTC) what can be explained with the hypothesis of tilted dipole (Curran and Rust, 1992), where the upper positive charge region is laterally displaced by the strong horizontal winds in middle and upper layers. In this situation the CG + strokes can originate from the upper positive charge region, because the shielding effect of the negative charge region in the middle layer is decreased. During the most intense increase of the total lightning activity in the period between 1530 UTC and 1535, the number of CG + strokes was slightly higher than the number of CG – strokes (Fig. 5a).

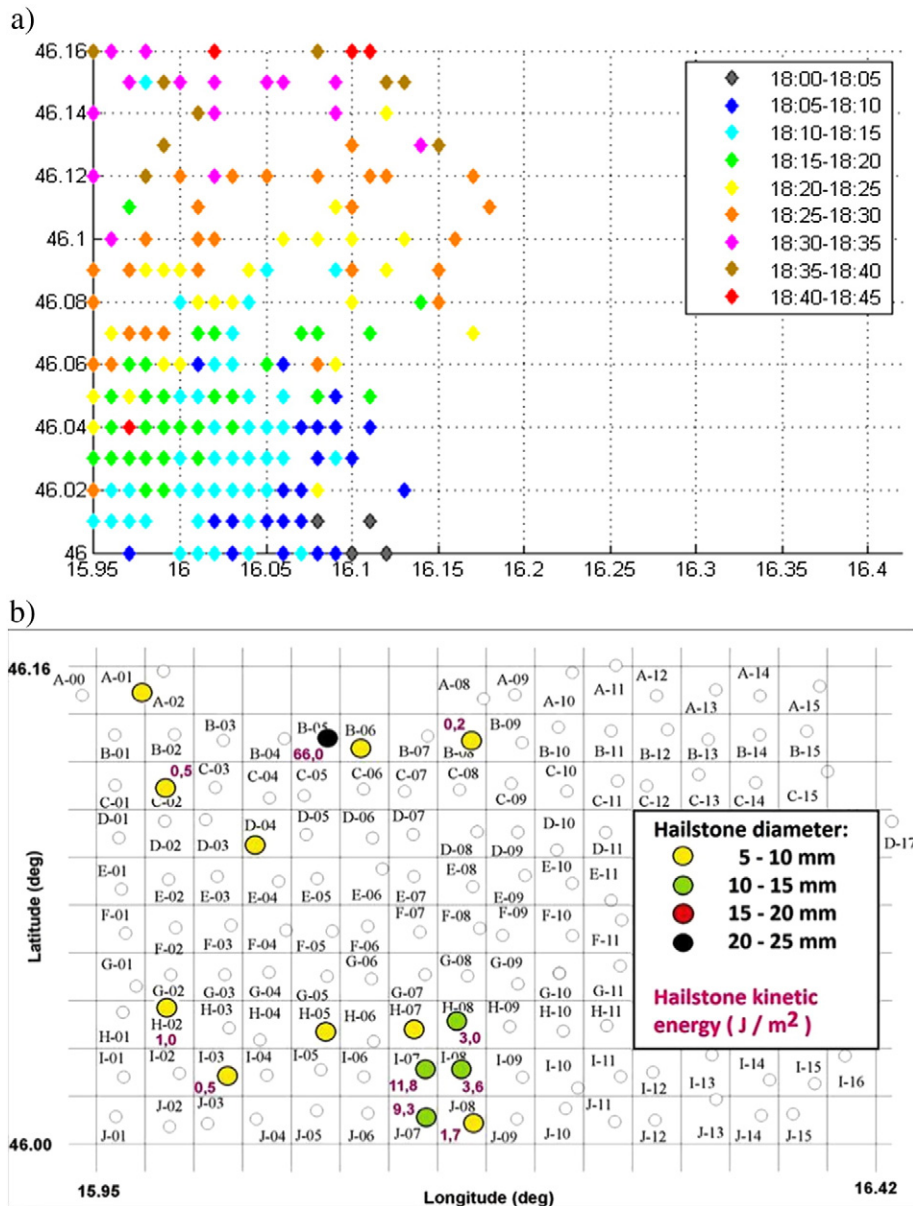


**Fig. 9.** Lightning strokes time/space distribution (a) and maximum hailstone size and kinetic energy distribution (b) for the hail case on 30 May 2008.

Contrary to numerous other studies (Carey and Rutledge, 2003; Montanya et al., 2007, 2009) in this lightning analysis no filtering of low peak currents was applied. In the previous studies the filtering was used because the lightning sensors usually misclassified the IC lightning as the CG lightning with peak currents lower than 10 kA. Summarized in Betz et al. (2004) the LINET sensors can detect much more CG strokes with low peak currents (<10 kA) compared to other lightning sensors. That is clearly shown when comparing the current amplitude distribution for different lightning networks (see Fig. 5.8 in Betz et al., 2004). According to their findings, LINET data show significant number of CG strokes with current amplitudes slightly lower than 10 kA. In order to compare the results with other studies, we have filtered out the CG strokes with peak currents lower than 10 kA (Fig. 5b). The result was that the IC lightning activity dominated over the CG lightning activity, what is in agreement with the previous studies (Montanya et al., 2007, 2009). The 96% of CG + strokes and 84% of CG – strokes in the studied storm had peak currents below 10 kA. The median of CG + current amplitude is 4.0 kA, while for CG – strokes it is –6.0 kA. The mean current (without filtering) for CG + (11 kA at 1500 UTC), CG – (16 kA at 1503 UTC) and IC (19 kA at 1500 UTC) strokes shows largest values at the beginning of the storm's lifecycle at around 1500 UTC (not shown) suggesting that the highest peak current values appear before the severe phase of the storm (Dimitrova et al., 2013). During the severe phase of the storm when the highest number of lightning strokes was detected, the mean current of lightning strokes was very low with the values lower than 8 kA (not shown). Additionally, detected lightning occurred well above the 12 km height (Fig. 4g–i), which was the height of the tropopause, as estimated from the sounding data of three closest radiosounding stations: Vienna, Budapest and Zagreb (not shown). The spatial distribution of these lightning discharges show a good correlation with the locations of the OT observed on the HRV images (Fig. 4a–c). Elliot et al. (2012) showed that certain

storms with OT produced a secondary maximum of lightning activity within or near the OT areas, which was associated with small regions of enhanced charging caused by an intense updraft within the thunderstorm. Support for this idea comes from the study by Emersic et al. (2011) who noted the occurrence of an upper maximum of lightning discharges detected during the analysis of hail-producing storms in Oklahoma, USA. In our case the mean height of IC strokes increased at the beginning of the convective storm and reached the maximum value of 14 km at 1513 UTC (Fig. 5c). During the mature phase of the convective storm the mean height was almost constant with the values between 11 and 12 km. After 1612 UTC the mean height started to decrease, representing the dissipating stage of studied cell. The IC strokes above 12 km had dominant positive polarity (Fig. 5d). The largest number of both positive and negative IC strokes was detected during the mature phase of convective cell with pronounced OT features at the storm tops in the period between 1530 UTC and 1615 UTC. It has to be mentioned that IC stroke polarities must be interpreted with caution, because the possibility of determination is strongly dependent on the channel orientation (Betz et al., 2004).

### 3.2. Comparison of lightning activity and hail properties in hail-producing storms

Complex microphysical processes including ice particles during hailstorms make the electrification process more intense, which consequently leads to more lightning activity in these convective clouds (Wiens et al., 2005; Petersen et al., 2005; Schultz et al., 2009). To assess the connection between lightning activity and hailfall, lightning characteristics were studied for hail-producing thunderstorms occurring over the hailpad polygon in the northwestern part of Croatia (Fig. 1b) from May to September 2008 to 2012. For all studied hailstorms the characteristic of hail such as start and end time of the hailfall, hailstone

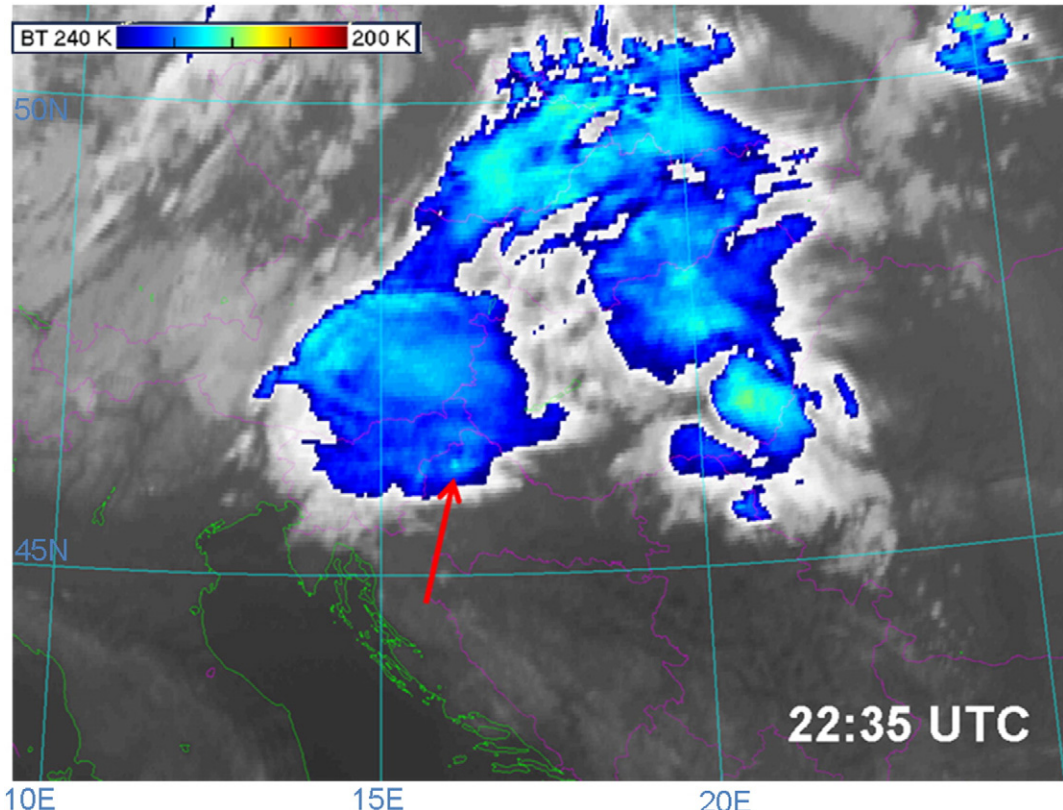


**Fig. 10.** Color-enhanced Meteosat 8 IR 10.8  $\mu\text{m}$  image for 11 July 2012 at 22:35 UTC. Red arrow marks a possible OT in the area of the hailpad polygon.

maximum diameter and kinetic energy are given in Table 1, together with the number of hailpads in the hailpad polygon on which the hail was registered. Additionally all storms were checked for specific cloud top features, such as OT, cold ring or cold U/V and their appearance is also marked in Table 1. The one of the goals of this research was to study lightning behavior during the severe storms which produced large hail (with diameter larger than 2 cm) and to check whether satellite characteristics of convective storm tops indicate the severe character of these storms.

In the majority of the studied cases, the number of total lightning strokes per minute sharply increased shortly before the beginning of hailfall. That is in agreement with previous studies which found a jump in a flash rate before the occurrence of hail at the ground (Williams et al., 1999; Dimitrova et al., 2013). Cases in which we did not find characteristic increase in lightning activity were the ones in which the produced hail had a diameter smaller than 1 cm and/or in which hail was registered on a smaller area over the polygon, usually on just one or two hailpads. At the time the hailfall started there was a brief decrease in the frequency of total lightnings, followed by a sharp increase shortly after. During the hailstorms which produced hail with diameter larger than 2 cm on satellite images the characteristics storm tops features such as OT, cold ring or cold U/V are detected (Table 1). On 30 May 2008, thunderstorms with very cold cloud-top temperatures, that were visible on the color enhanced IRW 10.8 μm satellite image, passed over the hailpad polygon. Using the “sandwich product” (Setvák et al., 2010; <http://www.convection-wg.org/sandwich.php>), HRV satellite images overlaid with color enhanced IRW 10.8 μm satellite images, the formation of the OT can be noted in the vicinity of the

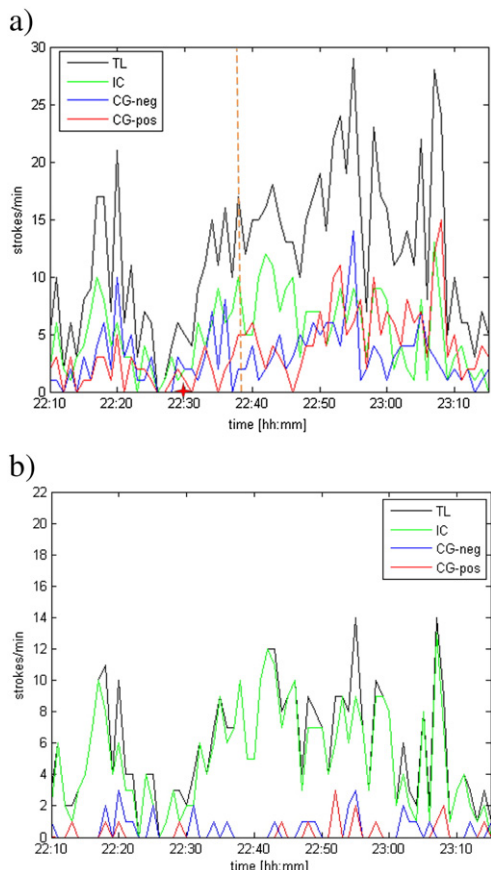


**Fig. 11.** Temporal distribution of a) lightning strokes (CG positive, CG negative, IC and TL) and b) filtered lightning strokes (CG positive > 10 kA, CG negative > 10 kA, IC and TL) on 11 July 2012. Dashed line indicates time of a small spot colder than the surrounding pixels on IR satellite imagery (Fig. 10) which likely represents an OT in the vicinity of the hailpad polygon. Star indicates beginning of the hailfall detected over the polygon (2230 UTC).

hailpad polygon at 1740 UTC (Fig. 6). Thirty minutes later in the color-enhanced IR 10.8 μm, a small cold ring feature can be observed (not shown).

Hail was registered at 13 hailpads between 1805 and 1835 UTC in the western part of the polygon. The time distribution of the total lightning strokes, but also CG +, CG – and IC strokes for the tracked convective storm that produced hail over the polygon are shown on Fig. 7a and b. The highest number of lightning strokes was recorded between 1800 and 1830 UTC with a pronounced peak between 1806 UTC and 1815 UTC (Fig. 7a). In the period between 1800 and 1810 UTC the convective storm with OT was detected on satellite images. The first increase in total lightning was in the period between 1741 UTC and 1745 UTC, what is approximately time of OT detected on satellite image from 17:40 UTC. During that hailstorm a significant number of CG – strokes (1929) were detected compared to the number of CG + strokes (743), especially in the period of hail falling (Fig. 7). 55% of these CG – lightning strokes had peak currents lower than 10 kA, with median of –8.8 kA and mean current of –11.77 kA (Fig. 7b). This storm shows continuous increase of the number of total lightning strokes and CG – strokes, as well as low number of CG + strokes during the lifetime what is not a typical lightning behavior for hailstorms according to the previous research (Soula et al., 2004). However, the severe character of the analyzed storm can be seen in Fig. 7, which shows a sharp increase of total lightning (Dimitrova et al., 2013), in particular CG – lightning strokes, just before the hail occurrence. During the whole lifetime of the analyzed convective cell the number of IC lightning strokes was quite low. However, in this case the hail was also detected over the polygon; one hailpad detected hail with diameter larger than 2 cm, while other hailpads detected hailstones with diameters between 0.5 and 1.5 cm (Fig. 9b). It can be noted that at 1805 UTC, when hail started to fall over the polygon, the number of CG – and total lightning strokes decreased (Fig. 7a). The largest values of mean current amplitudes for CG – (23 kA at 1756 UTC), CG + (34 kA at 1754 UTC) and IC (22 kA at 1736 UTC and 17 kA at 1756 UTC) strokes were detected before hailfall began (Fig. 8). The times of largest values of mean current for all three studied types of strokes correspond to the time of detected OT feature on satellite image from 17:40 UTC. During the hailfall (between 1805 UTC and 1830 UTC) the mean currents were rather low compared with the values before and after the hail falling.

A comparison of the lightning strokes time/space distribution (Fig. 9a) and maximum hailstone size and kinetic energy distribution (Fig. 9b) showed that the largest hailstones with diameters between 10 and 15 mm, and the highest values of kinetic energy (3.0–11.8 J m<sup>-2</sup>) fell at the beginning of the hailstorm from 1805 to 1810 UTC. During that hailstorm, the lightning increased from 25 strokes per 1 min to 92 strokes per 1 min in the 15 min between 1800 and

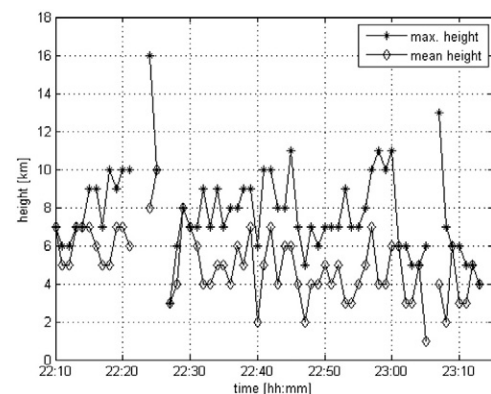


**Fig. 12.** Temporal distribution of maximum and mean height of IC lightning strokes on 11 July 2012.

1815 UTC (Fig. 7a). A rapid increase in the total lightning activity is an indication of sudden changes in the updraft mass flux through the mixed-phase region and could produce useful information for nowcasting the increased potential for severe weather (Schultz et al., 2009; Emersic et al., 2011).

The second hail-producing storm presents typical behavior of lightning activity in which the IC lightning production rate is higher than CG production rate during the lifetime of the hailstorm (Fig. 11) (Montanya et al., 2007, 2009). A color-enhanced IRW 10.8 μm image for 11 July 2012 shows a thunderstorm with relatively warm cloud tops, with cloud-top temperatures mostly higher than  $-40^{\circ}\text{C}$  (Fig. 10). The height of the tropopause estimated from the Zagreb radiosounding station at 12 UTC was  $\sim 9.5$  km (Fig. 14b), which justified rather warm cloud tops. A small spot colder than the surrounding pixels (Fig. 10) is marked by an arrow and likely represents an OT in the vicinity of the hailpad polygon. Since this was a nocturnal case, visual detection of the OT could not be performed in the HRV channel images. On the other hand, the OT detection in the IR satellite images or with objective detection methods is strongly dependent on thermo-dynamical properties of the storm (Setvak et al., 2008) and satellite temporal and spatial

resolution (Mikuš and Strelec Mahović, 2012b). Because of that, we could not be quite sure if and when the OT appeared at the top of this convective storm.

Hailstones with the largest diameter ( $>2$  cm) and highest values of kinetic energy (Fig. 13b) between 110 and  $160\text{ J m}^{-2}$  were registered at the beginning of the hailfall. Only the southernmost part of the storm over the polygon was bringing hail (Fig. 13b), although lightning was registered on a much broader area, which is seen in the image of time/space distribution of lightning strokes (Fig. 13a). The lightning production rate was lower (Fig. 11) compared to the previous example (Fig. 7), but rapid increase of the number of total lightning strokes was evident before the time of hail occurrence. From 2215 to 2220 UTC, the increase in total lightning frequency was detected (Fig. 11), after 10 min the hail was registered at the hailpad polygon. After 2240 UTC the lightning production rate increased, but the hail occurrence was not registered at the ground. Detailed analysis of lightning characteristics was performed for the period of the convective cell lifecycle when the hail was registered, between 2210 UTC and 2240 UTC. 85% of CG – and 93% of CG + lightning strokes had peak currents lower than 10 kA (Fig. 11b), with mean amplitude of  $-6.9$  kA for CG – and 5.8 kA for

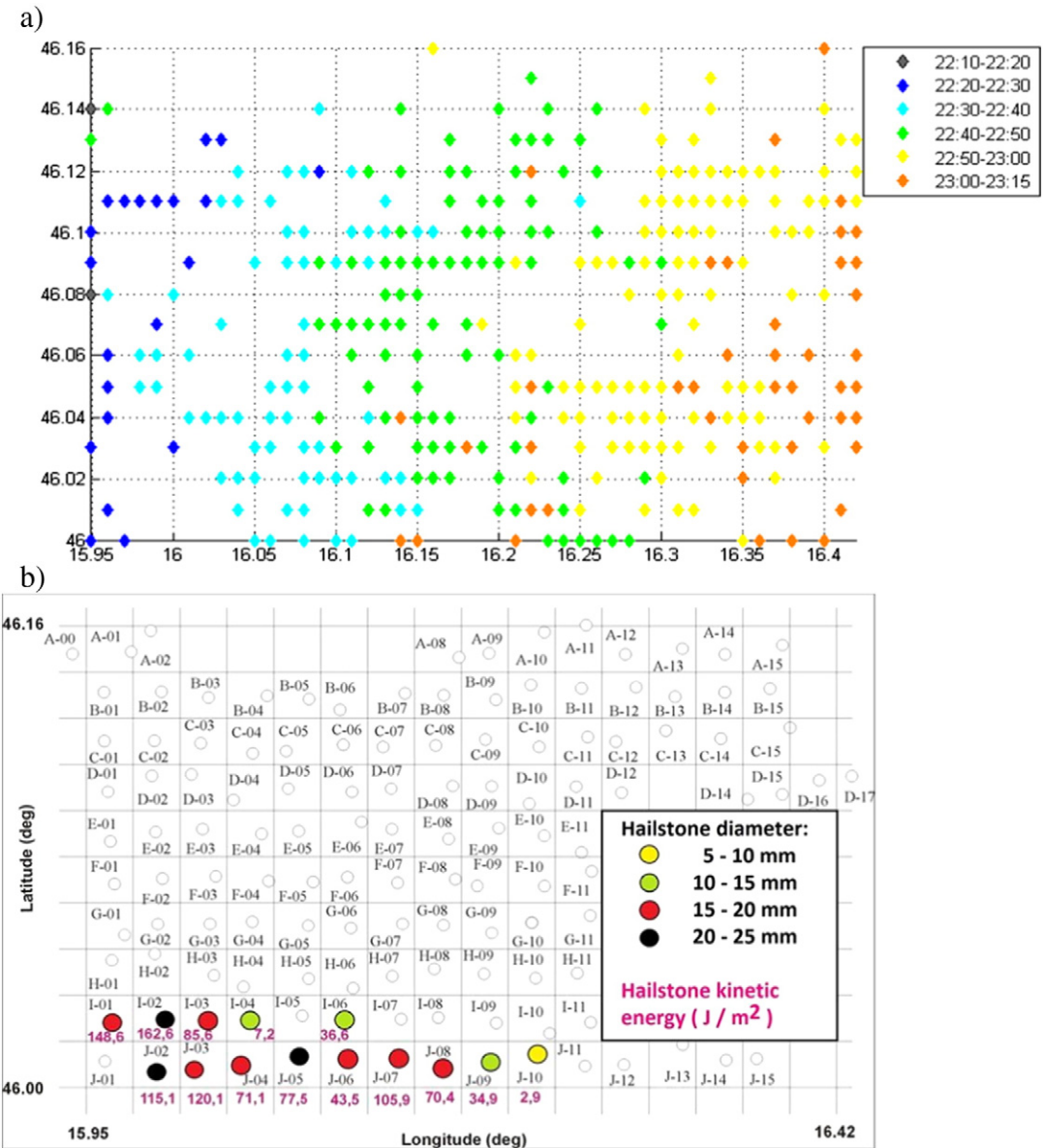
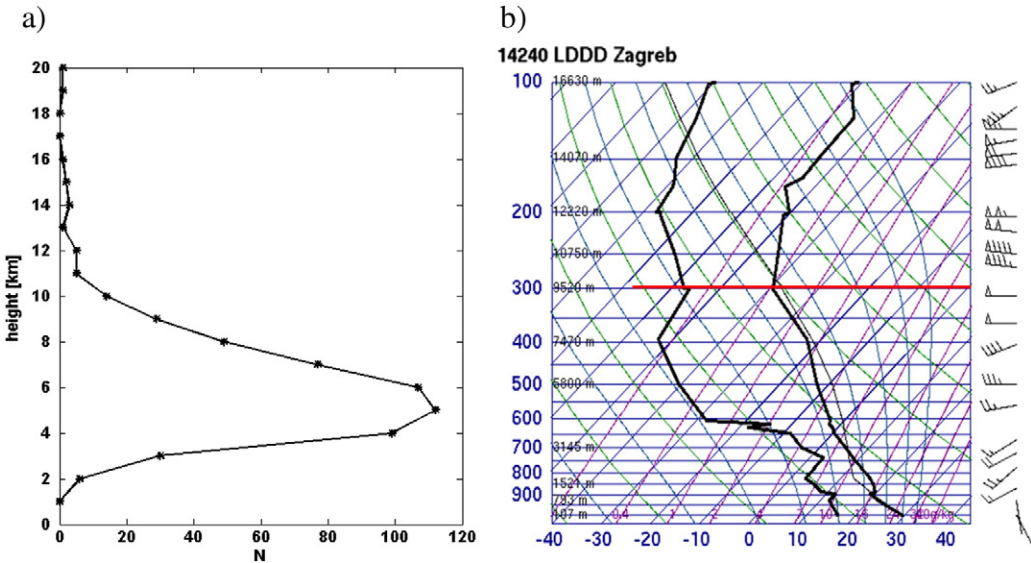


Fig. 13. Lightning strokes time/space distribution (a) and maximum hailstone size and kinetic energy distribution (b) for the hail case on 11 July 2012.



**Fig. 14.** a) Distribution of the number of lightning strokes with height for the hail case on 11 July 2012. b) Skew-T log-P diagram of radiosounding data from Zagreb on 11 July 2012 at 1200 UTC. The tropopause level is marked with the red line.

CG + strokes. The distribution of the lightning with height showed that the most IC lightning activity was observed between 4 and 7 km, with the peak at 5 km, which suggested that the storm tops were at low altitudes for a hailstorm (Fig. 14a). Although, the maximum and mean height of IC strokes was slightly higher before hail started to fall, with the peak values between 2224 UTC (maximum height = 16 km) and 2225 UTC (mean height = 10 km) (Fig. 12). That is in agreement with a study from Betz and Möhrlein, (2014), which found a significant increase in IC height before hail occurrence at the ground. They have shown that time evolution of IC height can be a very good indicator for severe weather, especially hail-producing storms.

### 3.2.1. Satellite-derived microphysical characteristics of hailstorm tops

Reflectivity information retrieved from the MSG SEVIRI 3.9  $\mu\text{m}$  channel is a measure of the cloud-top particle size, with higher reflectivity values for smaller cloud-top particles. When these small particles are found on top of cumulonimbus clouds with very cold cloud tops, it can be assumed that these particles did not have substantial time to grow in size, i.e., smaller particles at very low temperatures are an indication of strong updrafts. According to Lensky and Rosenfeld (2008), severe convective storms exhibiting strong updraft appear bright yellow in the “convective storms RGB” composite (an example of this composite is seen in Fig. 15a). This is because near zero 6.2–7.3 BTDS (regulating the red color) are found in the overshooting tops; large 3.9–10.8 BTDS (modulating the green color) are found in small ice particles at cloud tops, caused by homogenous freezing of cloud drops in strong updrafts (Rosenfeld et al., 2008), and large negative 1.6–0.6 reflectivity differences (modulating blue color of the RGB) are caused by the large absorption at 1.6  $\mu\text{m}$  by the ice particles (Strelc Mahović and Zeiner, 2009). Using properties of the 3.9  $\mu\text{m}$  reflectance and 10.8  $\mu\text{m}$  BT information, profiles of the T- $r_e$  were analyzed using the algorithm developed by Lensky and Rosenfeld (2006) for all cases of storms producing hail on the hailpad polygon in summer months from 2008 to 2012. The restriction applied to the T- $r_e$  analysis is the availability of the 3.9  $\mu\text{m}$  reflectivity information only during the daytime. Therefore, 20 cases were investigated (shaded gray in Table 1).

In almost all cases, T- $r_e$  profiles indicated the existence of small particles at low temperatures ( $r_e = 25 \mu\text{m}$  at  $-30^\circ\text{C}$ ,  $r_e = 30 \mu\text{m}$  at  $-40^\circ\text{C}$ ), which confirmed the presence of a moderate to strong updraft in the convective clouds. The profiles of particle growth with decreasing temperature (T- $r_e$  profiles) in all cases are comparable to the profiles

retrieved for the hailstorms by Rosenfeld et al., 2008 (see their Fig. 8b). Non-severe convective storms, on the other hand, have very different distribution of particle sizes with temperature, where large ice particles with  $r_e$  larger than 35  $\mu\text{m}$  are found already at temperatures around  $-20^\circ\text{C}$ , as shown in Rosenfeld et al. (2008) (see their Figs. 7 and 8a). The example in Fig. 15 shows the hail case in which 13 hailpads at the hailpad polygon detected hail of maximum diameter 18.2 mm and maximum kinetic energy  $47.7 \text{ J m}^{-2}$ . The duration of the hailfall over the polygon was about 20 min, from 1510 to 1530 UTC. The areas over which the T- $r_e$  profiles were generated are marked in Fig. 15a: a bigger “area 1” and a smaller “area 2”. The analysis of the T- $r_e$  profiles from the satellite reflectivity information requires a larger area, containing convective cells in different development phases, and is not directly related to a particular storm cell. In other words, the resulting profiles provide the information whether the air in the inspected area is prone to development of the storm with strong updraft or not. The corresponding profiles (Fig. 15b and c) suggest strong updraft existing over the area of interest ~10 to 20 min before the beginning of hailfall. In some cases Rosenfeld et al. (2008) report lead times of up to 90 min for the cases of tornado and large hail.

## 4. Summary and concluding remarks

An analysis of lightning activity in thunderstorms with OT was performed for the warm part of the year, May–September, during 2009 and 2010 and showed that the spatial distribution of lightning activity generally coincides with the spatial distribution of the detected OT. The temporal distribution showed that within the studied area, from approximately  $41^\circ\text{N } 8^\circ\text{E}$  to  $49.5^\circ\text{N } 20.5^\circ\text{E}$ , the largest number of OT with significant lightning activity was detected between 1630 and 1730 UTC, whereas from 0600 to 1000 UTC, both the lightning and OT were rare. In May, most of the intense lightning activity as well as the largest number of OT were detected over the continental part of the study area, whereas in the autumn, lightning and convective activity were more pronounced along the coastline and over the sea in association with increased mid-latitude cyclonic activity across this area. In the convective storms with the OT, cold ring or cold U/V features detected in the satellite images, number of total lightning strokes was greatly enhanced at the time of the overshooting. In order to compare the results with other studies (Montanya et al., 2007, 2009) we have filtered out the CG strokes with peak currents below 10 kA. Consequently, IC strokes dominated during

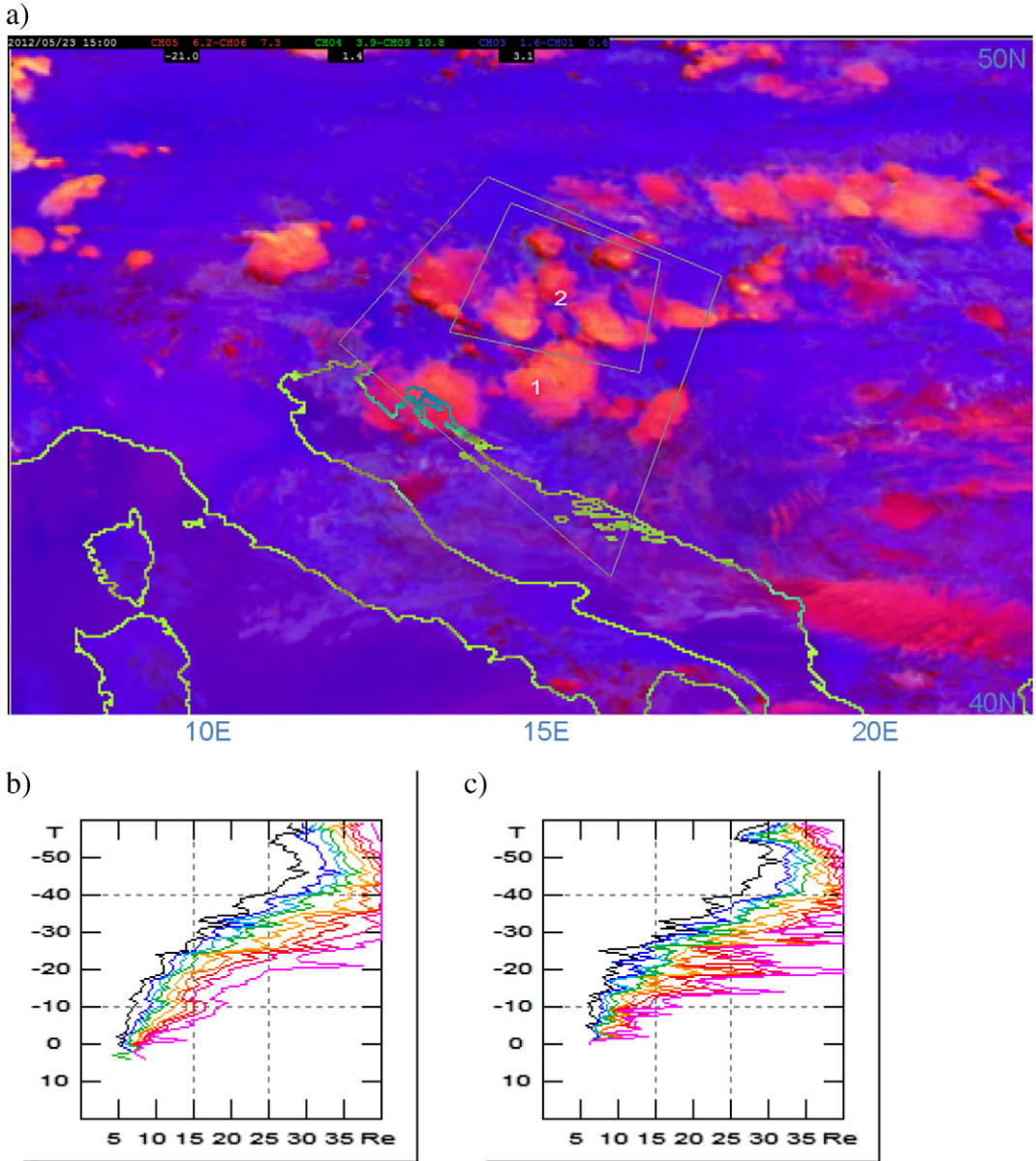


**Fig. 15.** a) METEOSAT 9 “Convective Storms” RGB composite (BTD 6.2–7.3  $\mu\text{m}$  defining red, BTD 3.9–10.8  $\mu\text{m}$  defining green and difference of reflectivities 1.6–0.6  $\mu\text{m}$  in blue) for 23 May 2012 at 15:00 UTC. Brighter 3.9  $\mu\text{m}$  reflectance (yellowish color in the RGB) means smaller cloud top particles. Polygons 1 and 2 denote the areas for which T-re profiles are being derived. b) and c) T-re analysis of the cloud top microstructure of the convective clouds in the polygons marked by 1 and 2, respectively. T-re profiles are derived from 3.9  $\mu\text{m}$  reflectivity and 10.8  $\mu\text{m}$  temperature data. The different colored lines represent different T-re percentiles every 5% from 5% (leftmost line) to 100% (rightmost line), where the green line presents the median.

the lifetime of the studied convective storms, leading to the conclusion that these storms produce a significant number of CG strokes with low peak currents. Because of that, results are strongly dependent on the detection efficiency of used lightning sensors (Betz et al., 2004). The temporal analysis of the mean current showed that the largest values appeared at the beginning of a storm's lifecycle, before the severe phase of the storm. That is in agreement with previous studies which have also found increase in peak currents before severe weather at the ground (Dimitrova et al., 2013). Moreover, IC lightning strokes occurred well above the tropopause; therefore, they are clearly related to the OT parts of the cumulonimbus cloud. Usually, the mean height of IC strokes had largest values at the time of OT detections, which is associated with larger number of IC strokes above the height of the tropopause (Elliot et al., 2012). These lightning characteristics could be used together with the satellite data for objective detection of the OT. Usually, all objective OT detection methods are satellite-based (Mikuš and Strelec

Mahović, 2012b), or combination of NWP model data and satellite data (Bedka et al., 2010). Satellite-based detection methods are strongly dependent on the spatial and temporal resolutions of the satellite data (Bedka et al., 2010), which are relatively coarse compared to the resolution of the lightning data. The findings from this research, in which we showed that in the case of the overshooting significant number of lightning strokes appear above the tropopause or at very high altitudes, could be used to improve the objective OT detection methods, which could potentially lead to more accurate nowcasting of severe storms.

For the hail cases that were recorded by the hailpads at the hail polygon, the number of total lightning strokes showed an increase slightly before hail occurrence at the ground. At the time the hailfall started, the number of total lightning strokes briefly decreased, followed by a sharp increase shortly after. In the cases with hailstone diameter lower than 1 cm and hail detected at very small area, with one or two hailpads, the characteristic increase in total flash rate was usually not

observed. The hailstorms which produced hailstones larger than 2 cm had OT, cold ring or cold U/V feature detected at the storm top. Also, in these convective storms a significant number of CG lightning strokes with peak currents below 10 kA were produced. The largest values of mean current for CG +, CG – and IC strokes were detected before the hailfall, while during the hailfall they were rather low compared to the values before and after hail falling. Also, the mean height of IC strokes showed an increase before hail was detected by hailpads and decrease during the hailfall. Additionally, larger hailstones with higher kinetic energy values appeared at the beginning of the hailshower. Profiles of the effective radii of cloud particles vs. temperature indicated that all studied hail-producing storms were storms with moderate to strong (even severe) updraft, indicative for hailstorms. The results clearly show that there is a strong connection between lightning characteristics and updraft strength, which is manifested in i) the appearance of the OT on top of the convective cloud, ii) timing of the hailfall and properties of the hail stones and iii) microphysical characteristics of the cloud tops observable in the satellite data.

In addition, satellite data were shown to be very powerful in the analysis of severe storms despite their rather low spatial resolution. The ability to detect strong updrafts by recognizing the OT and other features of the storm tops (using HRV and color-enhanced IR satellite images or objective satellite based detection methods) as well as microphysical properties of the cloud-top particles (T-re profiles) with significant lead times, makes these methods very useful in the nowcasting, with an important role especially in the areas lacking radar coverage. Lightning monitoring and detailed analysis of lightning data, combined with satellite-based methods during severe weather conditions, can improve the nowcasting of extreme weather events. However, in order to quantify the values of lightning jumps or the frequency of strokes above the tropopause during OT, a much larger number of storms should be analyzed. This already paves the path for the research that will follow.

## Acknowledgments

The authors would like to thank the Ministry of Science, Education and Sports of the Republic of Croatia for their support under the project "Storms and natural disasters in Croatia," Grant 004-1193086-3036. We would also like to express our gratitude to Dr. Daniel Rosenfeld from The Hebrew University in Jerusalem for providing the program for the calculation and visualization of the T-re profiles from MSG SEVIRI data. We would especially like to thank Prof. John R. Mecikalski and Prof. Hans D. Betz for useful suggestions and comments.

## References

- Anderson, G., Kliugmann, D., 2014. A European lightning density analysis using 5 years of ATDnet data. *Nat. Hazards Earth Syst. Sci.* 14, 815–829.
- Ávila, E.E., Bürgesser, R.E., Castellano, N.E., Collier, A.B., Compagnucci, R.H., Hughes, A.R.W., 2010. Correlations between deep convection and lightning activity on a global scale. *J. Atmos. Terr. Phys.* 72, 1114–1121.
- Bedka, K.M., 2011. Overshooting cloud top detections using MSG SEVIRI Infrared brightness temperatures and their relationship to severe weather over Europe. *Atmos. Res.* 99, 175–189.
- Bedka, K.M., Brunner, J., Dworak, R., Feltz, W., Otkin, J., Greenwald, T., 2010. Objective satellite-based detection of overshooting tops using infrared window channel brightness temperature gradients. *J. Appl. Meteorol. Climatol.* 49, 181–202.
- Betz, H.D., Moehrlein, M., 2014. All 3D technology – recognition of severe thunderstorms. *Meteorol. Technol. Int.* 80–82 (April).
- Betz, H.D., Schumann, U., Laroche, P. (Eds.), 2004. *Lightning: Principles, Instruments and Applications*. Springer (641 pp.).
- Betz, H.D., Schmidt, K., Laroche, P., Blanchet, P., Oettinger, W.P., Defer, E., Dziewit, Z., Konarski, J., 2009. LINET – an international lightning detection network in Europe. *Atmos. Res.* 91, 564–573.
- Black, R.A., Hallett, J., 1999. Electrification of the hurricane. *J. Atmos. Sci.* 56, 2004–2028.
- Boccippio, D., 2002. Lightning scaling relations revisited. *J. Atmos. Sci.* 59, 1086–1104.
- Bridenstine, P.V., Darden, C.B., Burks, J., Goodman, S.J., 2005. The application of total lightning data in the warning decision making process. Preprints, Conf. on Meteorological Applications of Lightning Data P1.2. Amer. Meteor. Soc., San Diego, CA ([Available online at <http://ams.confex.com/ams/pdfpapers/83037.pdf>]).
- Bruning, E.C., Rust, W.D., Schuur, T.J., MacGorman, D.R., Krehbiel, P.R., Rison, W., 2007. Electrical and polarimetric radar observations of a multicell storm in TELEX. *Mon. Weather Rev.* 135, 2525–2544. <http://dx.doi.org/10.1175/MWR3421.1>.
- Brunner, J.C., Ackerman, S.A., Bachmeier, A.S., Rabin, R.M., 2007. A quantitative analysis of the enhanced-V feature in relation to severe weather. *Weather Forecast.* 22, 853–872.
- Buechler, D.E., Blakeslee, R.J., Christian, H.J., Creasy, R., Driscoll, K., Goodman, S.J., Mach, D.M., 1996. Lightning activity in a tornadic storm observed by the optical transient detector. Preprints 18th Conference on Severe Local Storms. American Meteorological Society, San Francisco, CA (February).
- Buechler, D.E., Driscoll, K.T., Goodman, S.J., Christian, H.J., 2000. Lightning activity within a tornadic thunderstorm observed by the Optical Transient Detector (OTD). *Geophys. Res. Lett.* 27, 2253–2256.
- Carey, L.D., Rutledge, S.A., 1998. Electrical and multiparameter radar observations of a severe hailstorm. *J. Geophys. Res.* 103, 13979–14000.
- Carey, L.D., Rutledge, S.A., 2003. Characteristics of cloud-to-ground lightning in severe and nonsevere storms over the central United States from 1989–1998. *J. Geophys. Res.* 108 (D15), 4483. <http://dx.doi.org/10.1029/2002JD002951>.
- Christian, H.J., Blakeslee, R.J., Boccippio, D.J., Boeck, W.L., Buechler, D.E., Driscoll, K.T., Goodman, S.J., Hall, J.M., Koshak, W.J., Mach, D.M., Stewart, M.F., 2003. Global frequency and distribution of lightning as observed from space by the Optical Transient Detector. *J. Geophys. Res.* 108 (D1), 4005. <http://dx.doi.org/10.1029/2002JD002347>.
- Corman, L.B., Carmichael, 1993. Varied research efforts are under way to find means of avoiding air turbulence. *ICAO J.* 48, 10–15.
- Curran, E.B., Rust, W.D., 1992. Positive ground flashes produced by low-precipitation thunderstorms in Oklahoma on 26 April 1984. *Mon. Weather Rev.* 120, 544–553.
- Darden, C., Nadler, D.J., Carcione, B.C., Stano, G.T., Buechler, D.E., 2010. Utilizing total lightning information to diagnose convective trends. *BAMS* <http://dx.doi.org/10.1175/2009BAMS2808.1>.
- Dimitrova, T., Mitzeva, R., Betz, H.D., Zhelev, H., Diebel, S., 2013. Lightning behavior during the lifetime of severe hail-producing thunderstorms. *Q. J. Hung. Meteorol. Serv.* 117, 295–314.
- Dworak, R., Bedka, K.M., Brunner, J., Feltz, W., 2012. Comparison between GOES-12 overshooting top detections, WSR-88D radar reflectivity, and severe storm reports. *Weather Forecast.* 10, 1811–1822.
- Elliott, M.S., MacGorman, D.R., Schuur, T.J., Heinselman, P.L., 2012. An analysis of overshooting top lightning mapping array signatures in supercell thunderstorms. 22nd International Lightning Detection Conference, 2–3 April, Broomfield, Colorado, USA.
- Emersic, C., Heinselman, P.L., MacGorman, D.R., Bruning, E.C., 2011. Lightning activity in a hail-producing storm observed with phase-array radar. *Mon. Weather Rev.* 139, 1809–1825.
- Gatlin, P., 2006. *Severe Weather Precursors in the Lightning Activity of Tennessee Valley Thunderstorms.* (M.S. thesis), The University of Alabama in Huntsville (87 pp.).
- Gatlin, P.N., Goodman, S.J., 2010. A total lightning trending algorithm to identify severe thunderstorms. *J. Atmos. Ocean. Technol.* 27, 3–22.
- Höller, H., Betz, H.-D., Schmidt, K., Calheiros, R.V., May, P., Houngninou, E., Scialom, G., 2009. Lightning characteristics observed by a VLF/LF lightning detection network (LINET) in Brazil, Australia, Africa and Germany. *Atmos. Chem. Phys.* 9, 7795–7824.
- Iršič Žibert, M.I., Žibert, J., 2013. Monitoring and automatic detection of the cold-ring patterns atop deep convective clouds using Meteosat data. *Atmos. Res.* 123, 281–292.
- Iršič Žibert, M., Strajnar, B., Žibert, J., 2010. Cold-ring pattern on satellite images as indication of severe weather. Proc. 2010 EUMETSAT Meteorological Satellite Conf. EUMETSAT, Cordoba, Spain.
- Lane, T.P., Sharman, R.D., Clark, T.L., Hsu, H.M., 2003. An investigation of turbulence generation mechanisms above deep convection. *J. Atmos. Sci.* 60, 1297–1321.
- Lang, T.J., Rutledge, S.A., 2002. Relationships between convective storm kinematics, precipitation, and lightning. *Mon. Weather Rev.* 130, 2492–2506.
- Lang, T.J., Rutledge, S.A., Dye, J.E., Venticinque, M., Laroche, P., Defer, E., 2000. Anomalously low negative cloud-to-ground lightning flash rates in intense convective storms observed during STERAO-A. *Mon. Weather Rev.* 128, 160–173.
- Lensky, I.M., Rosenfeld, D., 2006. The time-space exchangeability of satellite retrieved relations between cloud top temperature and particle effective radius. *Atmos. Chem. Phys.* 6, 2887–2894.
- Lensky, I.M., Rosenfeld, D., 2008. Clouds–aerosols–precipitation satellite analysis tool (CAPSAT). *Atmos. Chem. Phys.* 8, 6739–6753.
- Lynn, B.H., Yair, Y., Price, C., Kelman, G., Clark, A.J., 2012. Predicting cloud-to-ground and intracloud lightning in weather forecast models. *Weather Forecast.* 27, 1470–1488.
- MacGorman, D.R., 1993. Lightning in tornadic storms: a review. In: Church, C., Burgess, D., Doswell, C., Davies-Jones, R. (Eds.), *The Tornado: Its Structure, Dynamics, Prediction and Hazards*. Geophysical Monograph vol. 79. American Geophysical Union.
- MacGorman, D.R., Rust, W.D., Schuur, T., Biggerstaff, M.E., Straka, J., Ziegler, C.L., Mansell, E.R., Bruning, E.C., Kuhlman, K.M., Lund, N., Helldson, J., Carrey, L., Eack, K., Beasley, W.H., Krehbiel, P.R., Rison, W., 2008. TELEX: the thunderstorm electrification and lightning experiment. *Bull. Am. Meteorol. Soc.* 89, 997–1013.
- Machado, L.A.T., Lima, W.F.A., Pinto, O., Morales, C.A., 2009. Relationship between cloud-to-ground discharge and penetrative clouds: a multichannel satellite application. *Atmos. Res.* 93, 304–309.
- Maddox, R.A., Howard, K.W., Dempsey, C.L., 1997. Intense convective storms with little or no lightning over central Arizona: a case of inadvertent weather modification? *J. Appl. Meteorol.* 36, 302–314.
- Manzato, A., 2007. The 6 h climatology of thunderstorms and rainfalls in the Friuli Venezia Giulia Plain. *Atmos. Res.* 83, 336–348.
- Meyer, T.C., Lang, T.J., Rutledge, S.A., Lyons, W.A., Cummer, S.A., Lu, G., Lindsey, D.T., 2013. Radar and lightning analyses of gigantic jet-producing storms. *J. Geophys. Res. Atmos.* 118, 1–17.

- Mezeix, J.F., Doras, N., 1981. Various kinetic energy characteristics of hailpatterns in the Grossversuch IV experiment. *J. Appl. Meteorol.* 20 (4), 179–186.
- Mikuš, P., Strelec Mahović, N., 2012a. Satellite-based overshooting top detection methods and the analysis of correlated weather conditions. *Atmos. Res.* 123, 268–280.
- Mikuš, P., Strelec Mahović, N., 2012b. Satellite-based overshooting top detection methods and an analysis of correlated weather conditions. *Atmos. Res.* 123, 268–280.
- Mikuš, P., Telišman Prtenjak, M., Strelec Mahović, N., 2012. Analysis of the convective activity and its synoptic background over Croatia. *Atmos. Res.* 104/105, 139–153.
- Montanyà, J., Soulà, S., Pineda, N., 2007. A study of the total lightning activity in two hailstorms. *J. Geophys. Res.* 112, D13118. <http://dx.doi.org/10.1029/2006JD007203>.
- Montanyà, J., Soulà, S., Pineda, N., van der Velde, O., Clapera, P., Sola, G., Bech, J., Romero, D., 2009. Study of the total lightning activity in a hailstorm. *Atmos. Res.* 91 (2–4), 430–437.
- Perez, A.H., Orville, R.E., Wicker, L.J., 1997. Characteristics of cloud-to-ground lightning associated with violent tornadoes. *Weather Forecast.* 12, 428–437.
- Petersen, W.A., Christian, H.J., Rutledge, S.A., 2005. TRMM observations of the global relationship between ice water content and lightning. *Geophys. Res. Lett.* 32, L14819. <http://dx.doi.org/10.1029/2005GL023236>.
- Počakal, D., 2011. Hailpad data analysis for the continental part of Croatia. *Meteorol. Z.* 20 (4), 441–447.
- Rogers, R.H., Carey, L., Bedka, K., Fleeger, C., Feltz, W., Monette, S.A., 2013. Total lightning in a multi-sensor approach to the detection and forecasting of convectively induced turbulence. *AMS meeting, 05–10.01. 2013, Austin, TX.*
- Rosenfeld, D., Lensky, I.M., 1998. Satellite-based insights into precipitation formation processes in continental and maritime convective clouds. *BAMS* 79 (11), 2757–2476.
- Rosenfeld, D., Woodley, W.L., Lerner, A., Kelman, G., Lindsey, D.T., 2008. Satellite detection of severe convective storms by their retrieved vertical profiles of cloud particle effective radius and thermodynamic phase. *J. Geophys. Res.* 113, D04208. <http://dx.doi.org/10.1029/2007JD008600>.
- Scheusener, R.A., Jennings, R.C., 1960. An energy method for relative estimates of hail intensity. *Bull. Am. Meteorol. Soc.* 41, 372–377.
- Schmitz, J., Pili, P., Tjemkes, S., Just, D., Kerkmann, J., Rota, S., Ratier, A., 2002. An introduction to Meteosat Second Generation (MSG). *BAMS* 83, 977–992.
- Schultz, C.J., Petersen, W.A., Carey, L.D., 2009. Preliminary development and evaluation of lightning jump algorithms for the real-time detection of severe weather. *J. Appl. Meteorol. Climatol.* 48, 2543–2563. <http://dx.doi.org/10.1175/2009JAMC2237.1>.
- Schultz, C.J., Petersen, W.A., Carey, L.D., 2011. Lightning and severe weather: a comparison between total and cloud-to-ground lightning trends. *Weather Forecast.* 26, 744–755.
- Schulz, W., Cummins, K., Diendorfer, G., Dorninger, M., 2005. Cloud-to-ground lightning in Austria: a 10-year study using data from a lightning location system. *J. Geophys. Res.* 110, 1984–2012.
- Setvák, M., Lindsey, D.T., Rabin, R.M., Wang, P.K., Demeterová, A., 2008. Indication of water vapor transport into the lower stratosphere above midlatitude convective storms: Meteosat Second Generation satellite observations and radiative transfer model simulations. *Atmos. Res.* 89, 170–180.
- Setvák, M., Lindsey, D.T., Novák, P., Wang, P.K., Radová, M., Kerkmann, J., Grasso, L., Su, S.-H., Rabin, R.M., Št'astka, J., Charvat, Z., 2010. Satellite observed cold-ring-shaped features atop deep convective clouds. *Atmos. Res.* 97, 80–96.
- Soulà, S., Seity, Y., Feral, L., Sauvageot, H., 2004. Cloud-to-ground lightning activity in hail-bearing storms. *J. Geophys. Res.* 109 (D2), D02101. <http://dx.doi.org/10.1029/2003JD003669>.
- Státska, J., Setvák, M., 2008. Cloud top temperature and height product of the nowcasting SAF applied to tropopause-penetrating cold-ring shaped storms. *Proc. 2008 EUMETSAT Meteorological Satellite Conf., Darmstadt, Germany. EUMETSAT.*
- Steiger, S.M., Orville, R.E., Murphy, M.J., Demetriades, N.W.S., 2005. Total lightning and radar characteristics of supercells: insights on electrification and severe weather forecasting. *Preprints, Conf. on Meteorological Applications of Lightning Data P1.7. Amer. Meteor. Soc., San Diego, CA ([Available online at <http://ams.confex.com/ams/pdfpapers/84908.pdf>]).*
- Steiger, S.M., Orville, R.E., Carey, L.D., 2007. Total lightning signatures of thunderstorm intensity over north Texas part I: supercells. *Mon. Weather Rev.* 135, 3281–3302.
- Strelec Mahović, N., Zeiner, B., 2009. Application of Meteosat SEVIRI channel difference 0.6 μm–1.6 μm in convective cells detection. *Atmos. Res.* 93 (1–3), 270–276.
- Stull, R.B., 1988. *Boundary Layer Meteorology*. Kluwer Academic (666 pp.).
- Tessendorf, S.A., Wiens, K.C., Rutledge, S.A., 2007. Radar and lightning observations of the 3 June 2000 electrically inverted storm from STEPS. *Mon. Weather Rev.* 135, 3665–3681.
- Tuomi, T.J., Larjavaara, M., 2005. Identification and analysis of lightning in thunderstorms. *Meteorol. Soc.* 131, 1191–1214.
- Wang, P.K., 2007. The thermodynamic structure atop a penetrating convective thunderstorm. *Atmos. Res.* 83, 254–262.
- Wang, P.K., Su, S.-H., Setvák, M., Lin, H., Rabin, R.M., 2010. Ship wave signature at the cloud top of deep convective storms. *Atmos. Res.* 97, 294–302.
- Wiens, K.C., Rutledge, S.A., Tessendorf, S.A., 2005. The 29 June 2000 supercell observed during STEPS Part II: lightning and charge structure. *J. Atmos. Sci.* 62, 4151–4177.
- Williams, E.R., Boldi, B., Matlin, A., Weber, M., Hodanish, S., Sharp, D., Goodman, S., Raghavan, R., Buechler, D., 1999. The behavior of total lightning activity in severe Florida thunderstorms. *Atmos. Res.* 51, 245–265.